Wei *et al.*
*European Journal of Medical Research* (2025) 30:10
https://doi.org/10.1186/s40001-024-02245-0

European Journal of Medical Research

RESEARCH

Open Access

# Metabolomic and proteomic profiling of a burn-hemorrhagic shock swine model reveals a metabolomic signature associated with fatal outcomes

Bin Wei[1,2†], Jinguang Zheng[1†], Jiake Chai[1*], Jianxiang Huang[1], Hongjie Duan[1], Shaofang Han[1], Xiaolin Yang[3], Wenjia Zhang[3], Fangchao Hu[1], Yirui Qu[1], Xiangyu Liu[1], Tian Liu[1], Yushou Wu[1] and Yunfei Chi[1*]

## Abstract

**Background** Burn-hemorrhagic shock combined injury, a severe condition causing complex stress responses and metabolic disturbances that significantly affect clinical outcomes in both military and civilian settings, was modeled in swine to investigate the associated metabolomic and proteomic changes and identify potential biomarkers for disease prognosis.

**Methods** Eight clean-grade adult male Landrace pigs (4–5 months, average weight 60–70 kg) were used to model burn-hemorrhagic shock combined injury. Serum samples collected at 0 h and 2 h post-injury were analyzed using metabolomic and proteomic measurements. The metabolomic and proteomic data were processed through partial least squares–discriminant analysis (PLS–DA) and the KEGG enrichment etc. Furthermore, the integrate analysis of the metabolomic and proteomic data was generalized by canonical correlation discriminant analysis, and the correlation between metabolites and mortality of the swine model was predicted using a multiple linear regression model by Pearson analysis.

**Results** PLS–DA revealed a global shift in each of the metabolomic and proteomic profiles following injury. The levels of 87 signature metabolites including various types of amino acids, fatty acids and acyl-carnitines of different lengths, and many metabolites in the gluconeogenesis, glycolysis, and tricarboxylic acid (TCA) cycle are generally increased ($P < 0.05$) after injury and can be used as biomarkers. Pathways related to amino acids metabolism and TCA cycle were significantly enriched ($P < 0.01$). In proteome analysis, we found dramatically altered ($P < 0.05$) levels of matrix and red blood cell-related proteins, such as type I collagen and hemoglobin. Most importantly, we found that the markedly elevated ($P < 0.01$) succinic acid, glutaric acid, and malic acid are closely associated (r = 0.863, 0.861, and 0.821, respectively) with injury severity by Pearson analysis, and can predict mortality using a multiple linear regression model.

**Conclusions** The study provides compelling observations that burn-shock swine model undergoes dramatic changes in the acute phase and present a valuable panel for clinical use of prognosis.

†Bin Wei and Jinguang Zheng have contributed equally to this work and co-first authors.

*Correspondence:
Jiake Chai
cjk304@126.com
Yunfei Chi
chi_yunfei@126.com
Full list of author information is available at the end of the article

**Keywords** Burn-hemorrhagic shock combined injury, Organic acids, Amino acids, Matrix and RBC-related proteins

## Introduction

Trauma has become a leading cause of death for individuals under the age of 45, with a significant portion of these deaths attributed to traumatic hemorrhagic shock in China. From our first aid experiences, trauma is often accompanied by burns, especially in vicious deflagration incidents, such as the Kunshan and Tianjin Port explosion accident in 2014–2015 in China and explosions in modern battlefield as well. Traumatic hemorrhagic shock combined with severe burns, featured by concurrence of burn induced post-burn hypovolemia and post-traumatic blood loss, are much more critical and complicated conditions than burn or traumatic-shock alone [1–3]. These severe combined conditions progress rapidly and present a particular challenge for treatment in both military and civilian populations. However, the diagnosis of injury severity is currently mainly subjective, lacking a clinically relevant quantitative measure. Furthermore, no efficient and special clinical preventions or treatments are available.

During severe injuries, the combined injury of burn-hemorrhagic shock being a typical example, the body undergo dramatic changes in material and energy metabolism as well as in proteostasis. A more comprehensive understanding of the metabolomics and proteomic changes may open new avenues for diagnostic and treatment development. Metabolomics globally and quantitatively analyzes the body's metabolites that are mostly small molecules (< 1500 Da) and can be used as physiological or pathological indicators for developing new diagnostic tests [4–6]. Several studies have utilized metabolomics profiling to identify novel biomarkers associated with disease progression, mechanisms, and prognosis, [7–9]. Proteomics systematically characterizes the protein expression and their interactions, offering complementary information to metabolomics on the functional changes in response to pathological events [10]. Multi-omics data may provide valuable insights into the mechanisms and biological functions that may not be revealed in a single data set [10–12].

In this study, we constructed a swine model of burn-hemorrhagic shock combined injury, as swine have physiological characteristics and metabolic processes that closely resemble those of humans, making them an ideal model for studying trauma-induced metabolic and proteomic disturbances. Using mass spectrometry-based metabolomics and proteomics techniques, we analyzed the metabolic and protein disturbances in serum after injury. The omics data revealed dramatically disordered metabolism and proteostasis, providing valuable insights into the physiological changes in response to the combined injury. Furthermore, we developed a multi-indicator panel for early diagnosis of injury severity, consisting of three metabolites—succinic acid, glutaric acid, and malic acid. These metabolites were selected based on their strong correlation with burn injury severity, ranking as the top three among all metabolites and proteins analyzed.

## Materials and methods

### Establishment of swine model of burn-hemorrhagic shock combined injury

The experiments were conducted following the International Guiding Principles for Biomedical Research Involving Animals released by the CIOMS and received approval from the Institutional Animal Care and Use Committee at Chinese PLA General Hospital, with the ethics approval ID 2021KY033-KS001. The animal research adhered to the ARRIVE guidelines (https://arriveguidelines.org). Eight clean-grade adult male Landrace pigs bred by Beijing Vital Steps Biotechnology Co. Ltd, with production license numbers SCXK (Beijing) 2018-0011 and SYXK (Beijing) 2024-0027 were used. The pigs were 4–5 months and weighed between 60 and 70 kg. To ensure that the pigs were healthy and ready for the study, they were adaptively fed for 1 week after they were purchased. The temperature of animal room was maintained between 22 and 25° C and a circadian rhythm was of 12 h of light and 12 h of darkness. The pigs were given abrosia for 12 h and water for 6 h before the experiment, Anesthesia was administered intravenously using Zoletil 50 (0.1 ml/kg) before the operation. A deep vein double-lumen catheter was indwelled in the right internal jugular vein of each pig under the guidance of ultrasound, and a PICCO arterial catheter was indwelled in the left femoral artery under the guidance of ultrasound.

After anesthesia, 400 g napalm were smeared on the back of the pigs and then ignited to burn for about 35 s to obtain a III° burn of 30% of the total area of skin in each pig. Then, 20% of the total blood volume was released from the femoral artery catheter at a uniform speed within 30 min after the burn, and 10% of the total blood volume was released at a constant speed in the next 5.5 h. The total blood volume was calculated according

to 70 ml/kg. Serum samples were collected before injury and 2 h after injury, respectively, as pre-injury control group (eight cases) and post-injury 2-h group (eight cases). The monitor and intervention procedures for each pig continued for 6 h after injury, and pigs that survived at the end of 6 h were finally euthanized.

#### Collection of serum samples

Blood samples were collected at room temperature and then centrifuged to obtain serum. After the animal model was prepared, blood samples were collected 2 h before and after injury individually. Use a medical vacuum coagulation tube to draw blood samples in animal model, keep the sample at 4 °C for 30 min, centrifuge with 1000*g* at 4 °C for 10 min, and then collect the serum supernatant. Each sample was collected and immediately stored at − 80 °C.

#### Metabolomics LC–MS/MS analysis

Quantitative determination of small molecule functional metabolites was performed using ultra-performance liquid chromatography–tandem mass spectrometry (UPLC–MS/MS) (ACQUITY UPLC-Xevo TQ-S, Waters Corp., Milford, MA, USA). Samples were separated by hydrophilic interaction liquid chromatography (HILIC) and analyzed by ACQUITY UPLC BEH C18 1.7 μM VanGuard pre-column (2.1 × 5 mm) and ACQUITY UPLC BEH C18 1.7 μM analytical column (2.1 × 100 mm) columns. All standards were purchased from Sigma-Aldrich (St. Louis, MO, USA), Steraloids Inc. (Newport, RI, USA) and TRC Chemicals (Toronto, ON, Canada). The standard substances were weighed accurately, dissolved in water, methanol, sodium hydroxide solution (Sigma-Aldrich, 795429) or hydrochloric acid solution (Sigma-Aldrich, 258148), and prepared as a concentration of 5.0 mg/mL stock solutions, respectively. A calibration solution was prepared and mixed with an appropriate amount of each standard sample.

Formic acid (Mass Pure Grade, A117-50) was purchased from Sigma-Aldrich (St.Louis, MO, USA), methanol (Mass Pure Grade, A-456-4), acetonitrile (Mass Pure Grade, A955-4) and isopropanol (Mass Pure Grade, A461-4) were purchased from Thermo-Fisher Scientific (FairLawn, NJ, USA). Experimental ultrapure water was prepared for LC/MS from a Mill-Q reference ultrapure water system (Millipore, Billerica, MA, USA) equipped with a 0.22 μm filter.

To avoid degradation of samples, they were thawed in an ice bath and 20 μL of blood samples were added to the 96-well plate, and then the plate was transferred to an Eppendorf epMotion workstation (Eppendorf Inc., Humburg, Germany). 120 μl of ice-water pre-cooled methanol solution (containing internal standard) was added and vortexed vigorously for 5 min. The plates were centrifuged (4000*g*, 30 min) at 4 °C, and returned to the workstation. 20 μL of freshly prepared derivatization reagent was added to each well, the plate was sealed and placed at 30 °C for 60 min of derivatization. Furthermore, 330 μL ice-bathed 50% methanol solution was added to dilute the sample, and centrifuged at 4 °C (4000*g*, 30 min), 135 μL supernatant was drawn and transferred to a new 96-well plate, which of 10μL was added each as internal standard. Add the derivatized standard stock solution to the left well for serial dilution, and finally seal the plate for LC–MS analysis.

#### Processing of metabolomics data

Raw data files were generated by UPLC–MS/MS and processed using MassLynx software (v4.1, Waters, Milford, MA, USA), and peaks were integrated, calibrated and quantified for each metabolite. The iMAP platform (v1.0, Metabo-Profile, Shanghai, China) was used for component analysis plotting and statistical analyses. Partial least squares–discriminant analysis (PLS–DA) and orthogonal partial least squares–discriminant analysis (OPLS–DA) were performed. Variable importance in projection (VIP) scores were obtained from the OPLS–DA model. Metabolites with VIP ≥ 1 and $P < 0.05$ (univariate analyses were performed based on the normality of the data) were considered statistically significant and identified as potential biomarkers.

#### Processing of serum proteomics data

Proteomic analysis method has been described previously [13] and the same biological samples as metabolomics were used. All proteomic data analyzed for serum of burn-hemorrhagic shock combined injury swine model were obtained from the Proteome Xchange consortium (http://proteomecentral.proteomexchange.org) through the iProX partner repository, data set. The identifier is IPX0003225000. PLS–DA plots were generated using the R (version 4.4.2) package mixOmics (version 6.30.0).

#### Integration of multi-omics data

To integrate analysis of the metabolomics and proteomics data, the sparse generalized canonical correlation discriminant analysis was performed through the data integration analysis for Biomarker Discovery in the potential cOmponents (DIABLO) [14] in the R package mixOmics [15]. A generalized, supervised partial least squares approach was applied to integrate multiple data types on

the same biological sample and jointly identify key omics signatures on multiple data sets. Normalized metabolomics and proteomics data were log-transformed by DAIBLO before integration. Specifically, we evaluated the correlation between the 33 differential proteins identified through proteomics and the top 10 metabolites from the metabolomics analysis. Pearson correlation coefficients were used to perform the correlation analysis.

### Statistical analysis

A series of operations for data processing, interpretation and visualization were performed using the iMAP (v1.0; Metabo-Profile, Shanghai, China) platform. Two statistical analysis methods are widely used in metabolomic research: (1) multivariate statistical analysis, such as partial least squares–discriminant analysis (PLS–DA) and (2) univariate statistical analysis, including *t* test, Mann–Whitney–Wilcoxon (*U* test), variance analysis, correlation analysis, etc. The best choice of statistical method usually depends on the data and project goals.

## Results

Metabolomics and proteomics analyses were performed on serum from pigs after they were subjected to thermal injury for 45 s followed by hemorrhagic shock for 2 h, and results were compared with 0 h serum control. Raw data are reported in Tables 1 and 2.

### Non-targeted metabolomics data indicated organic acids and amino acids are major serum metabolites in swine model with burn-hemorrhagic shock combined injury

In the non-targeted metabolomics experiment, PLS–DA completely segregated the 2 h post-injury group(t3) and 0 h control group(t0) with component 1 explaining 32.1% of the variance and mostly describing the effects of the combined injury, and component 2 (11.2%) mostly explaining biological variability across samples (Fig. 1A). 194 metabolites were identified. The composition of average abundance of the metabolites in all samples is 51.88% organic acids, 36.22% amino acids, 6.01% fatty acids, 3.99% indoles and 1.89% others (Fig. 1B). Compared to 0 h serum control, relative abundance of organic acids increased from 36.89 to 58.75%, but amino acids decreased from 47.66 to 30.98% in the serum 2 h post-injury. Other components such as lipids including fatty acids and carnitines also decreased obviously (Fig. 1C). The result suggested organic acid, amino acids and lipids have remarkable alterations in burn-hemorrhagic shock swine model.

#### *Organic acids and amino acids are obviously upregulated post injury in swine model*

Univariate analysis showed that 118 metabolites were significantly altered after injury including 116 up-regulated and 2 down-regulated ($P<0.05$, log2fold change$>=0$) (Fig. 2A). Among them, the top nine most differential metabolites with the lowest *P* values include hydroxypropionic acid, lysine, tyrosine, 2-methylbutyroylcarnitine, leucine, proline, 2-hydroxybutyric acid, alanine and phenylalanine (Fig. 2B). Eighty-seven potential biomarkers were selected through the intersection of univariate and OPLS–DA analyses (VIP$\geq 1$ and $P<0.05$) (Fig. 2C). These potential biomarkers are illustrated in a heatmap (Fig. 2D) and a histogram (Fig. 2E). KEGG pathway analysis based on the 87 metabolites revealed that the pathways most affected by the injury were alanine, aspartate and glutamate metabolism, phenylalanine metabolism; aminoacyl-tRNA biosynthesis, valine, leucine and isoleucine biosynthesis and tricarboxylic acid (TCA) cycle ($P<0.01$) (Fig. 2F).

#### *Altered amino acid, glucose and fatty acid metabolism levels*

Early in the 1980s, several groups had found that amino acid metabolism altered extremely during burn injury. They found hyperaminoacidemia peculiarly for glycine, hydroxyproline, alanine, lysine, phenylalanine, and glutamine in the acute phase [16]. While the serums which were collected 2 h post the burn-hemorrhagic shock combined injury, conforming to the acute phase, were used in metabolomic analysis. The results showed alanine, lysine and phenylalanine were increased significantly to 2.4, 1.7, and 1.5-folds, respectively, in the serum 2 h post-injury compared with control ($P<0.001$). Glutamine was increased 1.2-folds that of the control group ($P=0.09$). However, glycine and hydroxyproline, were not found significantly increased. A set of histidine-related amino acids and dipeptides increased: 1-methylhistidine (1MH) increased 1.12-folds ($P<0.001$) and histidine increased 1.3-folds ($P<0.01$), anserine (β-alanyl-3-methylhistidine) increased 1.46-folds ($P<0.05$) and carnosine (beta-alanyl-L-histidine) increased 1.45-folds ($P<0.01$). The metabolomic data also showed other amino acids increased significantly, as listed in Table 1.

Furthermore, the injury group exhibited an increase in the metabolites of glycolysis, gluconeogenesis, and TCA pathways in the serum. Lactic acid and pyruvic acid were significantly increased in the serum to 3.44-folds ($P<0.01$) and 3.25-folds ($P<0.01$), respectively. Five out of eight TCA cycle intermediates were significantly higher in the injury serum with a 1.5~4.7-folds increment. Glucogenic amino acids such as alanine, threonine, asparagine, tyrosine, histidine, serine, proline and valine

**Table 1** Pathway and related metabolites

| Metabolite | Class | HMDB | KEGG | Uni_P | Uni_FDR | FC | log2FC | OPLSDA_VIP |
|---|---|---|---|---|---|---|---|---|
| Lysine | Amino acids | HMDB0000182 | C00047 | < 0.0001 | 0.0023 | 1.6999 | 0.7654 | 1.6568 |
| Histidine | Amino acids | HMDB0000177 | C00135 | 0.002 | 0.0146 | 1.3064 | 0.3856 | 1.3586 |
| Anserine | Peptides | HMDB0000194 | C01262 | 0.0319 | 0.059 | 1.461 | 0.5469 | 1.0396 |
| Sarcosine | Amino acids | HMDB0000271 | C00213 | 0.0078 | 0.0183 | 2.212 | 1.1453 | 1.5015 |
| Alanine | Amino acids | HMDB0000161 | C00041 | 2.0E-4 | 0.0043 | 2.3728 | 1.2466 | 1.5872 |
| Dimethylglycine | Amino acids | HMDB0000092 | C01026 | 3.0E-4 | 0.0043 | 1.7023 | 0.7675 | 1.0847 |
| Threonine | Amino acids | HMDB0000167 | C00188 | 3.0E-4 | 0.0043 | 1.4429 | 0.529 | 1.5587 |
| Homoserine | Amino acids | HMDB0000719 | C00263 | 0.0017 | 0.0134 | 1.4161 | 0.5019 | 1.5696 |
| Threonic acid | Carbohydrates | HMDB0000943 | C01620 | 0.0078 | 0.0183 | 2.5976 | 1.3772 | 1.4152 |
| Hydroxypropionic acid | Organic acids | HMDB0000700 | C01013 | < 0.0001 | 0.0023 | 2.292 | 1.1966 | 1.5164 |
| 3-Pyridylacetic acid | Pyridines | HMDB0001538 | NA | 0.0333 | 0.0609 | 1.4504 | 0.5365 | 1.0532 |
| Glycylproline | Peptides | HMDB0000721 | NA | 0.003 | 0.0183 | 1.6617 | 0.7327 | 1.0772 |
| Lactic acid | Organic acids | HMDB0000190 | C00186 | 0.0078 | 0.0183 | 3.4444 | 1.7843 | 1.7931 |
| Tyrosine | Amino acids | HMDB0000158 | C00082 | < 0.0001 | 0.0023 | 1.6041 | 0.6817 | 1.3667 |
| 3,4-Dihydroxyhydrocinnamic acid | Phenylpropanoids | HMDB0000423 | C10447 | 0.0078 | 0.0183 | 11.846 | 3.5663 | 1.1862 |
| Asparagine | Amino acids | HMDB0000168 | C00152 | 0.0013 | 0.0114 | 1.4857 | 0.5711 | 1.5543 |
| Phenylalanine | Amino acids | HMDB0000159 | C00079 | 3.0E-4 | 0.0043 | 1.5061 | 0.5908 | 1.4068 |
| Hydroxyphenyllactic acid | Phenylpropanoic acids | HMDB0000755 | C03672 | 0.0078 | 0.0183 | 6.7646 | 2.758 | 1.5763 |
| Aminoadipic acid | Amino acids | HMDB0000510 | C00956 | 0.0078 | 0.0183 | 4.0065 | 2.0023 | 1.539 |
| Glucaric acid | Carbohydrates | HMDB0000663 | C00818 | 0.0213 | 0.0436 | 2.1857 | 1.1281 | 1.0712 |
| 2-Hydroxy-3-methylbutyric acid | Fatty acids | HMDB0000407 | NA | 0.0078 | 0.0183 | 4.2251 | 2.079 | 1.5481 |
| Hippuric acid | Benzoic acids | HMDB0000714 | C01586 | 0.0078 | 0.0183 | 3.3227 | 1.7324 | 1.1314 |
| N-Acetyalanine | Amino acids | HMDB0000766 | NA | 0.0078 | 0.0183 | 2.1638 | 1.1136 | 1.4551 |
| Malic acid | Organic acids | HMDB0000156 | C00149 | 0.0078 | 0.0183 | 3.3713 | 1.7533 | 1.2769 |
| N-Acetyaspartic acid | Amino acids | HMDB0000812 | C01042 | 0.0078 | 0.0183 | 3.7724 | 1.9155 | 1.6237 |
| Ethylmethylacetic acid | SCFAs | HMDB0002176 | C18319 | 0.0078 | 0.0183 | 2.1974 | 1.1358 | 1.1647 |
| Phenylacetic acid | Benzenoids | HMDB0000209 | C07086 | 0.02 | 0.0413 | 1.6582 | 0.7296 | 1.0935 |
| Fumaric acid | Organic acids | HMDB0000134 | C00122 | 0.0391 | 0.0653 | 1.9317 | 0.9499 | 1.2434 |
| Glutaric acid | Organic acids | HMDB0000661 | C00489 | 0.0078 | 0.0183 | 2.3935 | 1.2591 | 1.4145 |
| Aconitic acid | Organic acids | HMDB0000072 | C02341 | 0.0078 | 0.0183 | 1.8058 | 0.8526 | 1.0299 |
| Azelaic acid | Fatty acids | HMDB0000784 | C08261 | 0.0078 | 0.0183 | 2.1017 | 1.0715 | 1.4924 |
| Ketoleucine | Organic acids | HMDB0000695 | C00233 | 4.0E-4 | 0.0051 | 2.1787 | 1.1234 | 1.4219 |
| 3-Methyl-2-oxopentanoic acid | Organic acids | HMDB0000491 | C00671 | 7.0E-4 | 0.0078 | 2.0575 | 1.0409 | 1.264 |
| Phenylpyruvic acid | Benzenoids | HMDB0000205 | C00166 | 0.004 | 0.0183 | 1.8692 | 0.9025 | 1.1237 |
| Methylmalonic acid | Organic acids | HMDB0000202 | C02170 | 0.0234 | 0.0455 | 3.5436 | 1.8252 | 1.0593 |
| 2-Hydroxyglutaric acid | Organic acids | HMDB0000606 | C02630 | 0.0078 | 0.0183 | 2.826 | 1.4988 | 1.6101 |
| Citrulline | Amino acids | HMDB0000904 | C00327 | 0.0078 | 0.0183 | 1.5066 | 0.5913 | 1.2296 |
| Gluconolactone | Carbohydrates | HMDB0000150 | C00198 | 0.0078 | 0.0183 | 3.7778 | 1.9175 | 1.391 |
| Glycolic acid | Organic acids | HMDB0000115 | C00160 | 8.0E-4 | 0.0079 | 1.4825 | 0.568 | 1.2414 |
| Proline | Amino acids | HMDB0000162 | C00148 | < 0.0001 | 0.0031 | 1.7594 | 0.8151 | 1.6542 |
| Erythronic acid | Carbohydrates | HMDB0000613 | NA | 3.0E-4 | 0.0043 | 2.006 | 1.0043 | 1.3394 |
| N-Acetylserine | Amino acids | HMDB0002931 | NA | 0.002 | 0.0146 | 2.1477 | 1.1028 | 1.5193 |
| 5-Aminolevulinic acid | Amino acids | HMDB0001149 | C00430 | 0.0098 | 0.0225 | 1.2028 | 0.2664 | 1.0404 |
| 2-Hydroxybutyric acid | Organic acids | HMDB0000008 | C05984 | 1.0E-4 | 0.0031 | 2.4536 | 1.2949 | 1.2858 |
| Glutaconic acid | Organic acids | HMDB0000620 | C02214 | 0.0078 | 0.0183 | 3.0337 | 1.6011 | 1.6293 |
| Isoleucine | Amino acids | HMDB0000172 | C00407 | 8.0E-4 | 0.0082 | 1.3943 | 0.4796 | 1.2132 |
| Leucine | Amino acids | HMDB0000687 | C00123 | < 0.0001 | 0.0031 | 1.5664 | 0.6475 | 1.5162 |
| Xylose | Carbohydrates | HMDB0000098 | C00181 | 0.0078 | 0.0183 | 4.4526 | 2.1546 | 1.4146 |
| Ribulose | Carbohydrates | HMDB0000621 | C00309 | 0.0078 | 0.0183 | 2.2466 | 1.1677 | 1.6622 |

**Table 1** (continued)

| Metabolite | Class | HMDB | KEGG | Uni_P | Uni_FDR | FC | log2FC | OPLSDA_VIP |
|---|---|---|---|---|---|---|---|---|
| Xylulose | Carbohydrates | HMDB0001644 | C00310 | 0.0078 | 0.0183 | 2.4485 | 1.2919 | 1.6865 |
| Rhamnose | Carbohydrates | HMDB0000849 | C00507 | 0.0015 | 0.0125 | 1.3822 | 0.4669 | 1.0717 |
| Fructose | Carbohydrates | HMDB0000660 | C02336 | 0.0078 | 0.0183 | 13.7015 | 3.7763 | 1.5829 |
| Norleucine | Amino acids | HMDB0001645 | C01933 | 3.0E-4 | 0.0043 | 1.6933 | 0.7599 | 1.1661 |
| Homovanillic acid | Phenols | HMDB0000118 | C05582 | 0.0078 | 0.0183 | 4.6104 | 2.2049 | 1.5924 |
| Isobutyric acid | SCFAs | HMDB0001873 | C02632 | 0.0037 | 0.0183 | 1.6657 | 0.7361 | 1.3231 |
| Malonic acid | Organic acids | HMDB0000691 | C00383 | 0.0024 | 0.0166 | 1.9239 | 0.9441 | 1.0982 |
| N-Methylnicotinamide | Pyridines | HMDB0003152 | NA | 0.0391 | 0.0653 | 1.8428 | 0.8819 | 1.0776 |
| Phenyllactic acid | Phenylpropanoic acids | HMDB0000779 | NA | 0.0078 | 0.0183 | 4.5178 | 2.1756 | 1.5021 |
| Maleic acid | Organic acids | HMDB0000176 | C01384 | 0.0391 | 0.0653 | 2.8169 | 1.4941 | 1.2066 |
| Adipic acid | Fatty acids | HMDB0000448 | C06104 | 0.0391 | 0.0653 | 1.8306 | 0.8723 | 1.0577 |
| Methylglutaric acid | Fatty acids | HMDB0000752 | NA | 0.016 | 0.0338 | 1.5096 | 0.5942 | 1.2828 |
| 3-Methyladipic acid | Fatty acids | HMDB0000555 | NA | 0.0078 | 0.0183 | 1.9561 | 0.968 | 1.2422 |
| Isocaproic acid | SCFAs | HMDB0000689 | NA | 4.0E-4 | 0.0049 | 1.7003 | 0.7658 | 1.3892 |
| Pyruvic acid | Organic acids | HMDB0000243 | C00022 | 0.0078 | 0.0183 | 3.2506 | 1.7007 | 1.7474 |
| Oxoglutaric acid | Organic acids | HMDB0000208 | C00026 | 0.0156 | 0.0333 | 1.5722 | 0.6527 | 1.0285 |
| Octanoic acid | Fatty acids | HMDB0000482 | C06423 | 0.0078 | 0.0183 | 2.4304 | 1.2812 | 1.3508 |
| Oxoadipic acid | Organic acids | HMDB0000225 | C00322 | 0.0078 | 0.0183 | 4.0046 | 2.0016 | 1.3622 |
| Succinic acid | Organic acids | HMDB0000254 | C00042 | 0.0078 | 0.0183 | 4.6999 | 2.2326 | 1.1898 |
| Propionylcarnitine | Carnitines | HMDB0000824 | C03017 | 0.0129 | 0.0288 | 1.7716 | 0.8251 | 1.0528 |
| Butyrylcarnitine | Carnitines | HMDB0002013 | C02862 | 0.0078 | 0.0183 | 2.3095 | 1.2076 | 1.6117 |
| 2-Methylbutyroylcarnitine | Carnitines | HMDB0000378 | NA | < 0.0001 | 0.0028 | 1.7975 | 0.846 | 1.6292 |
| Isovalerylcarnitine | Carnitines | HMDB0000688 | NA | 0.0078 | 0.0183 | 1.4795 | 0.5651 | 1.0965 |
| Glutarylcarnitine | Carnitines | HMDB0013130 | NA | 0.0078 | 0.0183 | 2.1229 | 1.0861 | 1.2875 |
| Adipoylcarnitine | Carnitines | HMDB0061677 | NA | 0.0078 | 0.0183 | 2.7774 | 1.4738 | 1.1988 |
| Octanoylcarnitine | Carnitines | HMDB0000791 | C02838 | 0.0234 | 0.0455 | 1.4486 | 0.5347 | 1.0828 |
| Decanoylcarnitine | Carnitines | HMDB0000651 | NA | 0.0078 | 0.0183 | 2.4804 | 1.3106 | 1.1968 |
| Dodecanoylcarnitine | Carnitines | HMDB0002250 | NA | 0.0078 | 0.0183 | 2.4415 | 1.2878 | 1.3299 |
| Tetradecanoylcarnitine | Carnitines | HMDB0005066 | NA | 0.0078 | 0.0183 | 2.2606 | 1.1767 | 1.5118 |
| Palmitoylcarnitine | Carnitines | HMDB0000222 | C02990 | 0.0078 | 0.0183 | 1.6273 | 0.7025 | 1.1423 |
| Oleylcarnitine | Carnitines | HMDB0005065 | NA | 0.0078 | 0.0183 | 1.7265 | 0.7878 | 1.096 |
| Linoleylcarnitine | Carnitines | HMDB0006469 | NA | 0.0078 | 0.0183 | 2.092 | 1.0649 | 1.1309 |
| Methylmalonylcarnitine | Carnitines | HMDB0013133 | NA | 0.0084 | 0.0194 | 1.7356 | 0.7954 | 1.2258 |
| SAH | Nucleotides | HMDB0000939 | C00021 | 0.0156 | 0.0333 | 1.1246 | 0.1694 | 1.4568 |
| Indolelactic acid | Indoles | HMDB0000671 | C02043 | 0.0078 | 0.0183 | 5.1025 | 2.3512 | 1.5361 |
| Indole-3-pyruvic acid | Indoles | HMDB0060484 | C00331 | 0.0078 | 0.0183 | 2.6464 | 1.404 | 1.1105 |
| gamma-Glutamylalanine | Peptides | HMDB0006248 | C03740 | 0.0078 | 0.0183 | 2.3586 | 1.2379 | 1.2476 |
| Imidazolepropionic acid | Imidazoles | HMDB0002271 | C20522 | 0.004 | 0.0183 | 1.739 | 0.7983 | 1.3296 |

also increased significantly to furnish the liver with more raw material for gluconeogenesis (Table 1).

Levels of the vast majority of the detected fatty acid and acylcarnitines (ACs) species, ranging from short-chain, medium-chain and long-chain, increased significantly, while free L-carnitine concomitantly decreased upon burn-shock injury. Apart from above mentioned amino acid and fat alterations, organic acids such as oxoadipic acid and methylmalonic acid related to amino acid metabolism were also significantly higher. All detected bile acids increased significantly, no matter primary or secondary bile acid, conjugated or unconjugated bile acid (Table 1).

**Table 2** Differential proteins identified in the proteomic analysis of serum from the burn-hemorrhagic shock swine model

| Rank | Gene symbol | Fold change | *P* value |
|---|---|---|---|
| 1 | COL1A2 | 829.4905135 | 0.021359575 |
| 2 | NUCB1 | 24.78414762 | 0.034537236 |
| 3 | COL1A1 | 19.33018589 | 0.026975125 |
| 4 | BLVRB | 12.46376207 | 0.0076821 |
| 5 | HBB | 11.16486016 | 9.09064E-05 |
| 6 | HBA | 10.86873756 | 2.50369E-05 |
| 7 | CA2 | 7.134852796 | 0.00043506 |
| 8 | LOC110258651 | 6.622451864 | 0.020537207 |
| 9 | FGL1 | 6.389124744 | 0.009023506 |
| 10 | COL3A1 | 4.194684164 | 0.024099774 |
| 11 | GSTP1 | 3.489059581 | 0.006098794 |
| 12 | FGG | 3.34070614 | 0.004222232 |
| 13 | CA1 | 2.925132382 | 0.03408571 |
| 14 | FOLR1 | 2.14649846 | 0.015122239 |
| 15 | FGB | 2.127911282 | 0.02066422 |
| 16 | CKM | 2.045537323 | 0.009144042 |
| 17 | FGA | 2.005627102 | 0.015091825 |
| 18 | PRDX2 | 1.942806812 | 0.018898188 |
| 19 | LOC100624077 | 1.855229114 | 0.019253793 |
| 20 | VWF | 1.663265937 | 0.00061749 |
| 21 | TNXB | 1.566114089 | 0.007138895 |
| 22 | LTF | 1.413241477 | 0.006078791 |
| 23 | HSPG2 | 1.284726863 | 0.043464745 |
| 24 | COLEC11 | 0.667632564 | 0.00511882 |
| 25 | KRT10 | 0.627345327 | 0.012969766 |
| 26 | CAP1 | 0.507228635 | 0.0277738 |
| 27 | F13A1 | 0.485126751 | 0.00443342 |
| 28 | MERTK | 0.297637064 | 0.012092167 |
| 29 | FN1 | 0.288177788 | 0.001420973 |
| 30 | PARVB | 0.248728721 | 0.012525976 |
| 31 | GLUL | 0.24520209 | 0.003133127 |
| 32 | VASP | 0.172221356 | 0.018553429 |
| 33 | CORO1C | 0.052726251 | 0.004257127 |

### Proteomic analysis of serum from swine model of burn-hemorrhagic shock combined injury

To establish a comprehensive view of burn-hemorrhagic shock combined injury, proteomics were performed based on the same serum samples. We identified totally 594 proteins after removing albumin, IgG, and other high-abundance proteins from the samples. PLS–DA revealed two distinct clusters, effectively discriminating between the serum proteomics of the 0 h control group and the 2 h post-injury group (Fig. 3A). Compared to the control, there were 33 differentially expressed proteins in the serum 2 h post-injury. Among them, 23 proteins were upregulated and 10 proteins were downregulated ($P<0.05$, |log2fold change|>=0.5) (Fig. 3B). The importance of response to wounding, coagulation, homeostasis, body fluid levels regulation, wound healing, cell-substrate adhesion, and platelet activation are emphasized by the Biological Process (BP) analysis. The extracellular region, extracellular space, extracellular exosome, extracellular organelle, extracellular vesicle, and collagen-containing extracellular matrix are enriched by Cellular Component (CC) analysis. Structural molecule activity, extracellular matrix structural constituent and cell adhesion molecule binding are enriched by Molecular Function (MF) analysis (Fig. 3C). Platelet activation, Focal adhesion, Complement ECM–receptor interaction and PI3K–Akt signaling pathway are regulated by KEGG analysis (Fig. 3D).

#### *Matrix and RBC-related proteins are increased in the serum of burn-shock group*

Two isoforms for type I collagen (COL1A1, COL1A2) were identified and both showed remarkable elevations in the serum 2 h post-injury. COL1A2 increased the most dramatically among all the differential proteins reaching an 829.49-folds ($P=0.02$), and COL1A1 ranks the third (19.3-folds, $P=0.02$). Collagen type III alpha-1 chain preproprotein (COL3A1) was identified and showed a 4.2-fold increase ($P=0.02$). Hemoglobin alpha and beta chains (HBA and HBB), the most abundant protein in RBC, displayed tenfold and 11-fold increment, ranking NO.6 and NO.5, respectively. Biliverdin reductase B (BLVRB) was upregulated as much as 12.5-fold ($P<0.01$) making the fourth strongest increment. Glutathione S-transferase P (GSTP1) was also identified and showed a 3.48-fold increase ($P<0.01$). Peroxiredoxin-2 (Fragment, PRDX2) showed a 1.9-fold ($P=0.01$) increment. Two isoforms for carbonic anhydrase (CA1, CA2) are increased 2.92-fold (P=0.03) and 7.13-fold ($P<0.001$), respectively (Table 2).

#### *Wounding, acute stress proteins and coagulation proteins are identified and altered*

Five proteins were identified in this category. Three isoforms of fibrinogen were detected as fibrinogen alpha, beta and gamma chains (FGA, FGB, FGG). Their quantitative rise hovered between 2 ~ threefold ($P<0.05$) in the serum 2 h post-injury. A stress associated protein, creatine kinase M-type (CKM) increased 2.05-fold ($P<0.01$). Serum coagulation factor XIII A chain (F13A1) was also identified in our samples and showed a twofolds decrease in the burn-shock group ($P<0.01$) (Table 2).

### Integrated correlation analysis of multi-omics data

Correlation analysis between injury-related metabolites and differential proteins identified that six metabolites were closely related to 13 differential proteins observed in the proteome which correlation > 0.7 (Fig. 4A). Type I

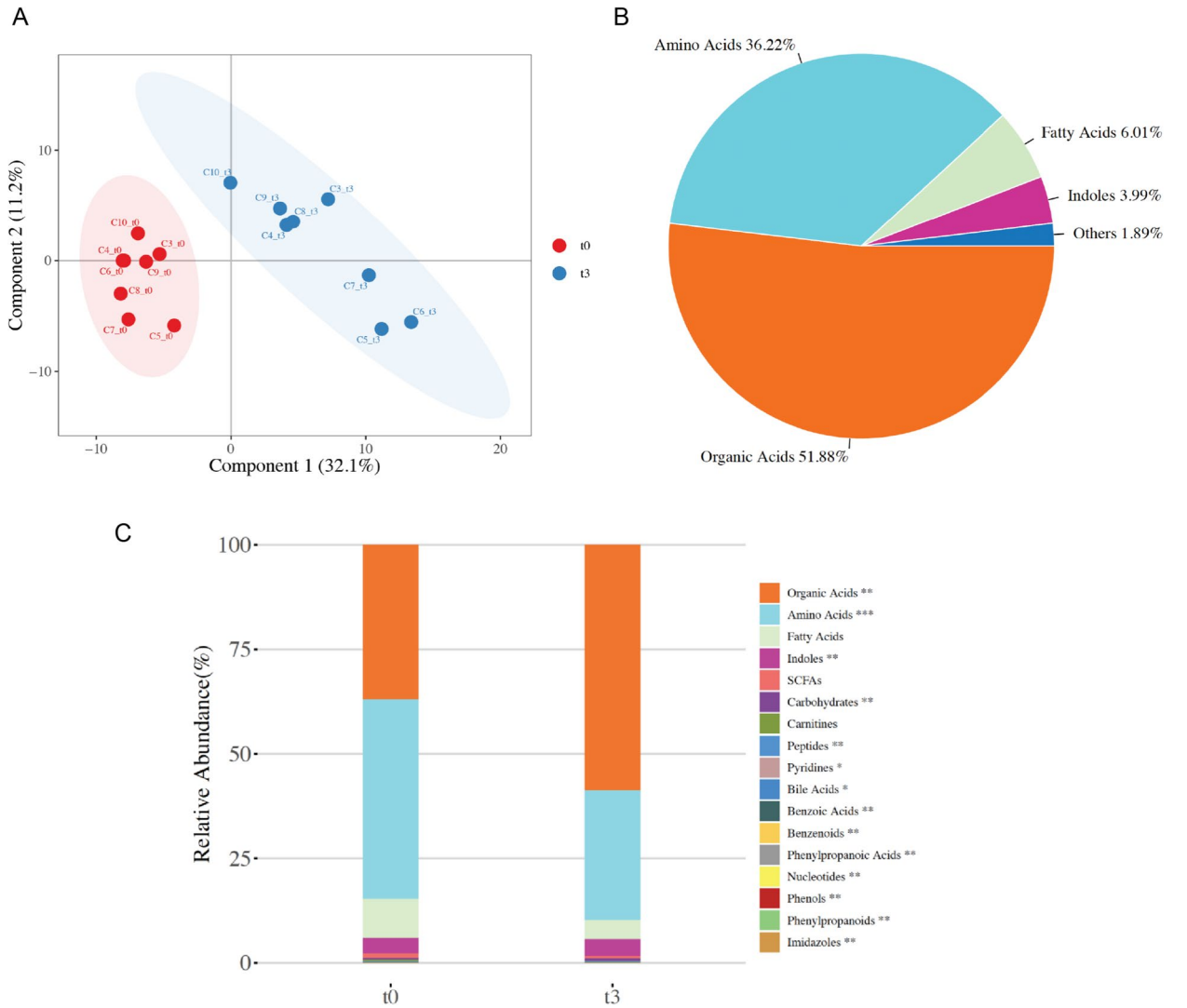


**Fig. 1** QC results of non-targeted metabolomics of serum metabolites in swine model. **A** Partial least-squares–discriminant analysis (PLS–DA) of all samples with a multivariate dimensionality-reduction tool; **B** Pie chart of the class distribution of detected metabolites; **C** Serum composition at 2 h post-injury (t3) shows increased organic acids and decreased amino acids and lipids compared to baseline (t0)

collagen is strongly associated with malic acid, glutaric acid, methylmalonic acid, and succinic acid; hemoglobin is strongly associated with threonine and succinate. CA was strongly associated with pyridineacetic acid, aminoadipic acid, glucaric acid, phenylacetic acid, citrulline, ALA, and 2-hydroxybutyric acid (Fig. 4B). Therefore, in burn-hemorrhagic shock combined injury the potential components of the two omics data sets are highly correlated.

### Succinic acid, glutaric acid and malic acid levels are associated with injury severity and can predict fatal outcomes

Injury scores were determined depending on the survival time of the pigs after injury to reflect injury severity. Three pigs out of eight were still alive 6 h post-injury and were assigned injury degree 1 (mild disease); two pigs died 4 h post-injury and were assigned degree 2 (moderate disease); Three pigs died 2 h post-injury and were assigned 3 (severe disease). Pearson correlation analysis was performed between the injury score and the elevated value of each differential metabolite and protein (serum value of the differential metabolite or protein at 2 h minus that at 0 h). Ten metabolites and three proteins were found to demonstrate significantly positive linear correlation with injury scores ($P < 0.05$) (Table 3). Succinic acid, glutaric acid and malic acid showed the highest Pearson correlation coefficients. We further performed biostatistical methods to analyze whether the

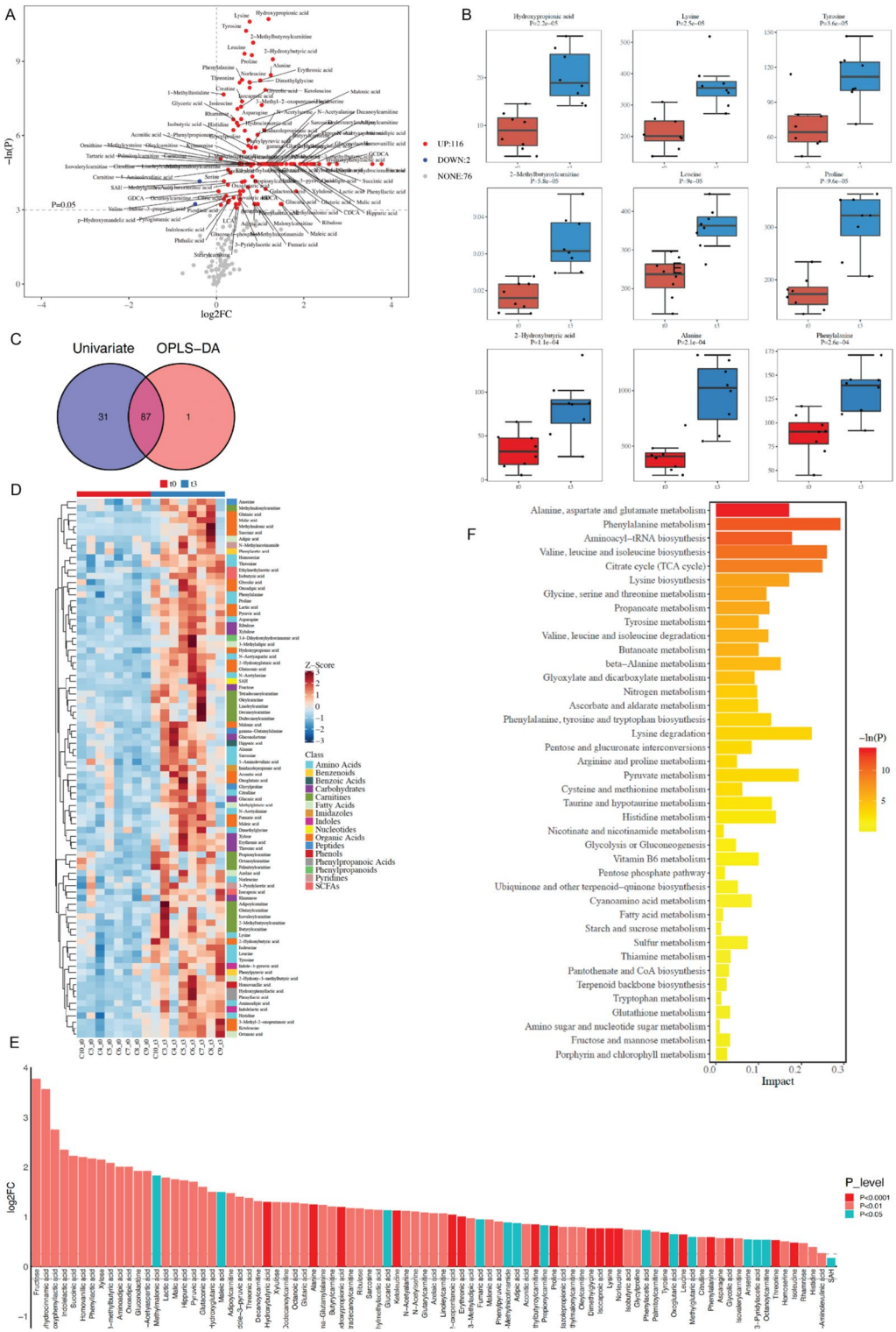


**Fig. 2** Differential changes of metabolites and pathways were analyzed for non-targeted metabolomics of serum metabolites in swine model. **A** Volcano plot of all differential metabolites with labels; **B** boxplot of the top nine most differential metabolites with the lowest *P* values between the 0 h control group (t0) and the 2 h post-injury group (t3), showing individual data points; **C** Venn diagram of differential metabolites identified by univariate and OPLS–DA analyses; **D** heatmap of the indicated differential metabolites; **E** Bar plot of Log2FC and *P* values for the indicated metabolites; **F** bar plot of KEGG pathway analysis based on fold enrichment

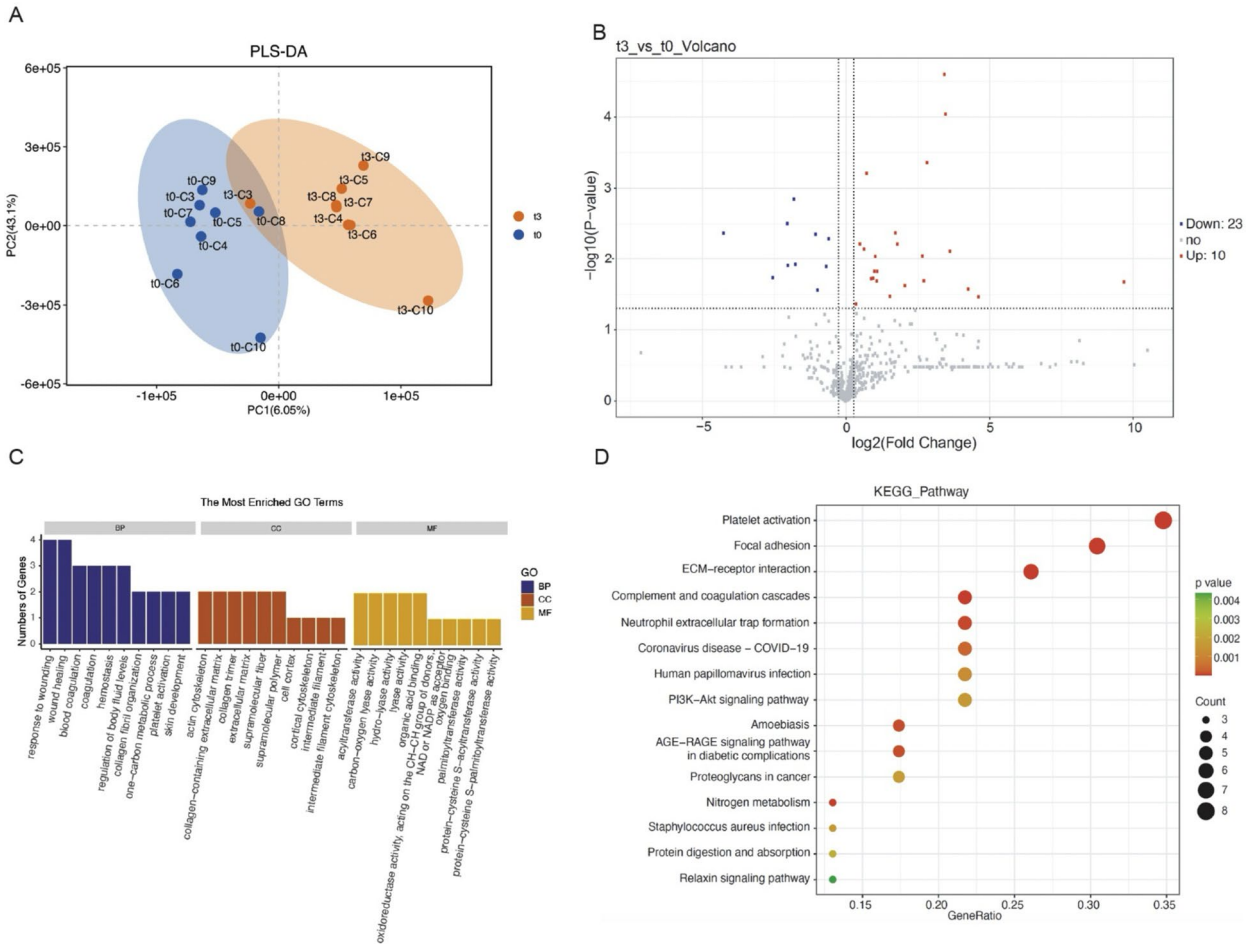


**Fig. 3** Proteomic analysis of serum from the swine burn-hemorrhagic shock combined injury model. **A** Partial least squares–discriminant analysis (PLS–DA) of the serum proteomics data of the 0 h control group (t0) and the 2 h post-injury group (t3). **B** Volcano plot of all differential proteins; **C** enrichment GO terms with biological process (BP), CC and MF; **D** KEGG pathway analysis

elevated serum levels of succinic acid, glutaric acid and malic acid together, were linked to fatal outcomes. Using multiple linear regression analysis, we get an equation combining the three variants to predict the degree of injury severity. The model generated the coefficients to identify the injury severity degree (Table 4). The regression line effectively determines the appropriate values for the intercept and slope, resulting in a line that best fits the given criteria. The prediction formula can be described as "Injury Severity = 0.998735 + 0.007335 × Δ(succinic acid) + 1.355171 × Δ(glutaric acid) + 0.01229 × Δ(malic acid)". Δ(succinic acid), Δ(glutaric acid), and Δ(malic acid) represent the net differences in their concentrations, calculated as the post-injury levels minus the pre-injury levels. The intercept (0.998735) reflects the baseline injury severity when there is no measurable net differences in the metabolite levels. The coefficients indicate the magnitude of each metabolite's contribution to the predicted injury severity. The model, with a coefficient of determination ($R^2$) of 0.8025, explains approximately 80.25% of the variability in injury severity, indicating that it is a robust predictor. Additional metrics, such as the mean absolute error (MAE), mean squared error (MSE), and root mean squared error (RMSE), further confirm the model's predictive accuracy and robustness (Table 4). Comparisons between actual and predicted values (Fig. 5A, B) demonstrate the model's high performance in capturing the relationship between metabolite alterations and injury severity. In addition, we used Q–Q Residuals to show the reliability of our linear regression model (Fig. 5C). The distribution of the residues revealed the model's excellent performance.

Our results suggest a potential therapeutic strategy that would involve decreasing serum levels of above metabolites and proteins, especially succinic acid, glutaric acid and malic acid, during severe burn-hemorrhagic shock injuries. We also suggest that levels of succinic acid,

A

| Row | Column | correlations |
|---|---|---|
| GSTP1 | Anserine | 0.714 |
| HBB | Threonine | -0.952 |
| HBA | Threonine | -0.881 |
| LOC100624077 | Threonine | 0.714 |
| COL1A2 | Malic acid | 0.929 |
| COL1A1 | Malic acid | 0.929 |
| COL1A2 | Glutaric acid | 0.810 |
| COL1A1 | Glutaric acid | 0.810 |
| COL1A2 | Methylmalonic acid | 0.786 |
| COL1A1 | Methylmalonic acid | 0.786 |
| COL1A2 | Succinic acid | 0.786 |
| COL1A1 | Succinic acid | 0.786 |
| HBB | Succinic acid | -0.738 |

B

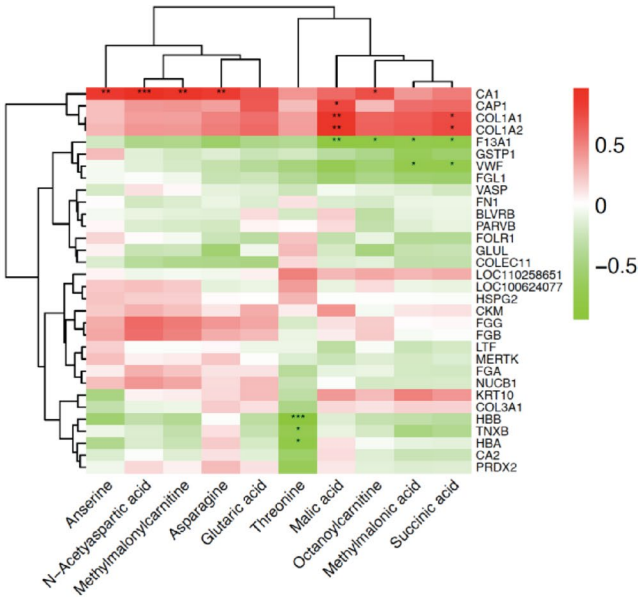


**Fig. 4** Integrated analysis of multi-omics data. **A** Correlation analysis between injury-related metabolites and differential proteins observed in the proteome which correlation > 0.7. **B** Heatmap of correlations between the potential components of the two omics data sets in the burn-hemorrhagic shock combined injury model

**Table 3** Metabolites and proteins demonstrating significantly positive linear correlation with injury scores

| | Name | *P* | Cor |
|---|---|---|---|
| Differential metabolites | Succinic acid | 0.006 | 0.863 |
| | Glutaric acid | 0.006 | 0.861 |
| | Malic acid | 0.012 | 0.821 |
| | Methylmalonylcarnitine | 0.017 | 0.800 |
| | Octanoylcarnitine | 0.025 | 0.788 |
| | Methylmalonic acid | 0.025 | 0.771 |
| | N-Acetyaspartic acid | 0.030 | 0.768 |
| | Anserine | 0.047 | 0.766 |
| | Threonine | 0.048 | 0.761 |
| | Asparagine | 0.048 | 0.755 |
| Differential proteins | COL1A2 | 0.030 | 0.757 |
| | COL1A1 | 0.040 | 0.729 |
| | CA1 | 0.045 | 0.718 |

glutaric acid and malic acid in the serum consist an indicator panel of disease severity and can predict mortality.

## Discussion

Burn and hemorrhage shock patients often exhibit severe hemodynamic disturbance, hypermetabolism, oxidative stress and stimulation of catabolic hormone. To globally examine the molecular and biochemical changes in the body, we constructed a swine model of burn-hemorrhagic shock combined injury and examined the changes in global metabolic and proteomic profiles in serum following injury. Despite the preliminary studies in burn or shock alone, to the best of our knowledge, no metabolomics and proteomics studies of the burn-hemorrhagic shock combined injury has been published to date. Swine models are selected, because they are better than rats in burn and shock studies, showing much more related metabolomic changes with human during injury.

A series of metabolic and proteomic biomarkers are discovered for burn-hemorrhagic shock combined injury; furthermore, a total of 13 important differential metabolites

**Table 4** Multiple linear regression prediction model

| Data set | Intercept | Coefficient | Score (R2) | Mean absolute error (MAE) | Mean squared error (MSE) | Root Mean squared error (RMSE) |
|---|---|---|---|---|---|---|
| Metabolites | 0.998735 | [0.007335, 1.355171, 0.012291] | 0.8025119 | 0.3204862 | 0.1481161 | 0.3848585 |

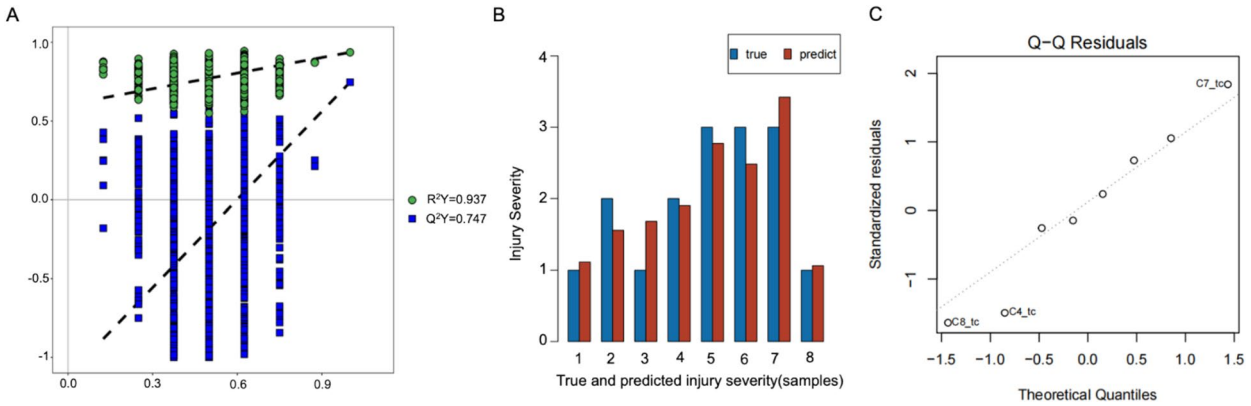


**Fig. 5** Serum levels of succinic acid, glutaric acid and malic acid levels are linked to injury severity and predicted fatal outcomes by biostatistical methods. **A** Permutation tests of PLS–DA models for the correlation coefficients; **B** actual and predicted values in both data sets; **C** a residuals vs. fitted, Q–Q residuals, scale-location and residuals vs. leverage to test linear regression models

and proteins are found to be correlated with injury degree, which can be used as biomarkers to evaluate the severity of injuries, and provide a strategy for early diagnosis and intervention of patients who may deteriorate.

### Altered amino acid, glucose, fatty acid metabolism and related potential treatments

Severe burn and shock trauma causes profound stress response early after the trauma. During stress, glucocorticoid and catecholamines are rapidly and profoundly increased in the circulating blood, which exert significant effects on whole-body protein, glucose and lipid metabolism, characterized by hyperglycemia (increased glycogenolysis and gluconeogenesis, and decreased glycogenesis) and hypercatabolic state with loss of collagen and muscle mass leading to profound skeletal muscle wasting shown in previous studies [16, 17]. We found similar but more comprehensive and extensive changes in the metabolomic data in the combined injury.

### Decreased mitochondria oxidation and CoQ10

Long before the utilization of mass spectrum in metabolites analysis, deuterated and carbon-labeled stable isotopes of glucose has been used to quantify glucose metabolism in burned adults. These studies have shown the percentage of glucose cleared into tissue that was fully oxidized to CO2 was lower, suggesting a deficit in glucose oxidation in tissue of burned patients [18, 19]. Galster et al. also reported that muscle lipid oxidation following burns is depressed [20, 21]. Many studies have tried to found what makes the severely burned patient unable to oxidize glucose and lipid efficiently as energy sources. Early in 2007, Cree et al. found that mitochondrial oxidation of both glucose and palmitate in tissue of burn patients were reduced to only about half of controls [20]. Providing additional powerful evidence, in our metabolome data, we detected significant accumulation of pyruvic acid, kinds of FFAs and acyl-carnitines in the serum 2 h post injury. Glucose and fat oxidation pathways converge at acetyl CoA that finally enter a common TCA cycle, suggesting a dysfunction in this common process in burn [22]. Furthermore, five out of the eight TCA intermediates, that is, citric acid, oxoglutaric acid, succinic acid, fumaric acid, and malic acid, were found significantly accumulated in the serum 2 h post-injury, suggesting the TCA cycle are somehow severely blocked. TCA cycle is followed by electron transport chain (ETC) to transfer the electrons from NADH to O2 in mitochondria innermembrane. The three heavily regulated key enzymes in TCA cycle, citric acid synthase, isocitric acid dehydrogenase and α-ketoglutarate dehydrogenase can be inhibited by high $NADH/NAD^+$ ratio. Therefore, electron transfer rate is critical for TCA cycle turn over. In cases of ETC complex damage or serious hypoxia, electron of NADH cannot be transferred to $O_2$ to produce $H_2O$, which leads to the blockade of ETC and subsequent increase in the ratio of $NADH/NAD^+$. TCA cycle is then blocked. Integrating all these information, we proposed that the increased glucose, fat and TCA intermediates are due to a block in the ETC.

In accordance with our hypothesis, succinate accumulation has been associated with increased mortality following hemorrhagic shock (HS) in military [23] and civilian [24] populations. One explanation is that HS cause oxygen scarcity in tissue, which subsequently exacerbate mitochondrial uncoupling [25]. Another explanation relies on the excess glutaminolysis that provide a rate-limiting substrate for the synthesis of hemorrhagic succinate in RBC [26]. However, the suppression of glutaminolysis by glutaminase inhibitor unexpectedly

exacerbated the HS rat, suggesting that increased succinate is not from glutamine or glutaminolysis [27].

We then propose that the reversal of the blocked ETC–TCA can reduce the increased glucose, fat and TCA intermediates and improve the prognosis of severe burns-hemorrhagic shock injury. Coenzyme Q10 (CoQ10) can enhance the function of ETC and promote oxidative phosphorylation reactions [28], protecting the integrity of cell membranes and mitochondrial membranes. Previous studies reported that CoQ10 supplementation could effectively prevent mitochondrial dysfunction and insulin resistance of skeletal muscle caused by burns [29, 30]. PPAR-α agonists is another candidate, since it can increase mitochondrial function and fatty acid oxidation by increasing citric acid synthase activity and up-regulating expression of many genes for proteins involved in substrate oxidation, including enzymes involved in the TCA cycle and respiratory chain [31].

#### Decreased glycolysis and increased gluconeogenesis

In our study, we detected 3.25-fold increment for pyruvic acid. Pyruvic acid is a core metabolite in glucose metabolism. Totally, pyruvic acid has four fates, converting to acetyl CoA, lactate, alanine and oxalacetate, respectively. Traumatic stress induced glucocorticoid can inhibit the oxidation of pyruvic acid to form acetyl CoA. Together with the blocked TCA cycle, the levels of pyruvic acid and the other products of pyruvic acid, such as lactate and alanine, increased in our study. However, oxalacetate was not detected in neither the 0 h nor the 2 h post-injury serum. One possible reason maybe that the increased NADH/$NAD^+$ ratio will promote malic acid formation from oxalacetate. The other reason is that oxalacetate can be converted to phosphoethanopyruvic acid to form glucose. During the burn-hemorrhagic shock stress, the gluconeogenesis pathway increased under regulation of highly increased glucocorticoid; therefore, oxalacetate level decreased. As the increased alanine would inhibit pyruvate kinase, and increased citric acid can inhibit phosphfructokinase-1, the glycolysis level was supposed to be greatly inhibited in the burn-hemorrhagic shock combined injury.

#### Increased lipolysis, decreased carnitine transportation and L-carnitine

Stress hormones, such as epinephrine, are potent activators of adipose tissue lipolysis, and could mobilize lipid in fat tissue to release more free fatty acids into blood after the severe trauma. FFA uptaken into cells will be first changed to acyl CoA in cytosol, and then transported into mitochondria via the mitochondrial carnitine/acylcarnitine shuttle transport system, and β-oxidized to acetyl CoA. We detected significantly increased medium chain fatty acids and short-, medium- and long-chain acyl-carnitines, together with an exhausted free carnitine pool. It has been proposed that acute elevations in lipolysis responding to adrenergic stress may increase energy availability accomplishing an adaptive response [32]. However, our data suggest that the acetyl CoA cannot enter TCA efficiently because of the TCA–ETC blockade. Then, the acyl-carnitines accumulated because of the inability to cycle and release free carnitine. Taken together, these data offer a convincing explanation as to why glucose and lipid taken up by tissue is not fully oxidized by mitochondria.

In the injured group, significantly increased levels of succinic acid, oxoglutaric acid, as well as lysine are involved in carnitine synthesis pathway and are in agreement with the increased demand for L-carnitine synthesis, suggesting that L-carnitine supplementation can potentially maintain and restore normal metabolic levels. Downregulation of L-carnitine in serum has been reported to inhibit the activity of pyruvate dehydrogenase, causing the accumulation of pyruvic acid [33]. In addition, it also indirectly affects amino acid metabolism [34]. L-carnitine is now used clinically to alleviate hemorrhagic shock, reduce ischemia and hypoxia. It has also been reported that L-carnitine supplementation can reduce cellular and mitochondrial damage in the liver by maintaining CPT1 enzyme activity [35]. Yet, it is important to note that speeding up of the TCA–ETC is indispensable to avoid the supplemented L-carnitine being trapped in the acyl-carnitine step.

#### Insulin resistance

Previous studies [36] showed that elevated concentrations of short- and long-chain acylcarnitines, which are also detected in our study (Table 1), have been linked to insulin resistance. Together with above data of decreased glycolysis, increased gluconeogenesis, our results indicate the development of insulin resistance, providing a much detailed and comprehensive glucose and fat metabolite profile.

#### Protein alteration and related potential treatments

##### *Increased matrix protein*

Collagen is the most abundant protein in mammals, approximately accounting for one-third of the whole-body protein. It has been reported early in the 1960's that the administration of cortisol to rats resulted in induction of collagenolytic and proteolytic activities in the extracellular compartment of the skin with marked and abrupt loss of cutaneous collagen [37]. Thermal injury also

destructed collagen into amino acids [16]. Correspondingly, our proteomic examination found the type I collagen increased significantly in the serum 2 h post-injury compared with control and correlate with the degree of injury severity. Notably, the true identity of the "collagen" shown in the proteome may be not the complete length protein, but is the peptides produced from collagen breakdown during connective tissue destruction, and further mapped to collagen during LS–MS analysis. Glycine and hydroxyproline present in large amount in collagen; however, they were not found significantly increased in our metabolome data. These results suggest that the collagens may be degraded not only into amino acids as reported early [16], but also into peptide segments, especially during the acute phase within 2 h post-injury.

#### *Altered RBC-related proteins*

Recent studies have estimated that the adult human body contains 25 trillion circulating RBCs accounting for ~ 83% of all host cells. This makes RBCs a type of circulating organ critical for human health and the damage and hemolysis is supposed to play important roles in both physiological and pathological situations [38, 39]. In our injury model. We found important signs of hemolysis, which may influence the prognosis.

Oxidative response is crucial for the maintenance of normal function and integrity of RBCs [40, 41]. Several diseases such as favism with deficiency of GADH activity have underlined their importance. Reactive oxygen species (ROS) can cause RBCs damage, but a diversity of antioxidant systems is known to protect and repair RBCs. The high-capacity redox systems in RBC also scavenge extracellular radicals and thus protects against radicals formed in the body as a whole [40].Under normal steady-state conditions, the very solid protection systems against ROS can cope with the threat. However, during the extensive oxidative stress induced by the severe burn and shock trauma, abundant ROS are released and significantly reduce the antioxidative capacity of RBCs and damage them. Massive hemolysis is subsequently induced releasing appreciable amounts of cytosol contents into the circulation. Each mature RBC contains ~ 250–270 million copies of hemoglobin, accounting for ~ 98% of the cytosolic proteome [42]. This is in accordance with our proteomic data of presence of large amounts of free hemoglobin in blood in the combined injury.

Other proteins that present abundantly in RBCs, such as BLVRB, glutathione transferase, peroxiredoxin, and carbonic anhydrase (CA) were also significantly increased 2 h post-injury. Antioxidant proteins are expressed in high abundance in mature RBCs to help regulate cellular redox. BLVRB is a general NADPH-dependent flavin reductase (FR) that reduces numerous substrates, and plays a critical role in regulating cellular redox. Wu et al. found BLVRB mRNA levels increased during erythropoiesis [43] and Paukovich et al. detected high levels of BLVRB in mature RBCs through mass spectrometry analysis, confirming the importance of BLVRB in redox regulation [44]. Glutathione transferase P1-1 (GSTP1-1) is abundant in mammalian RBCs and is exclusively expressed during erythropoiesis. GSTP1-1 detoxify a large variety of toxic compounds using glutathione or by acting as a ligandin, and is also involved in the oxidative stress. GSTP1-1 has been found overexpressed in the human erythrocyte in the case of increased blood toxicity, such as in healthy subjects living in polluted areas and is likely a defense response to increased blood toxicity [45]. Peroxiredoxin 2 (Prdx2) is the third most abundant protein present in RBCs and acts as a quick sink of peroxides by reacting with them to generate a disulfide-linked dimer [46]. By the correlation analysis, CA1 increment could predict the degree of injury severity suggesting a relationship between hemolysis and severity of injury. Similarly, previous researches have shown that free hemoglobin in burn blister fluid reflected burn severity [41]. Taken together, the increases in RBC-related proteins in the serum 2 h post-injury support an important role of hemolysis in the progress of the combined injury.

### Multivariate linear regression model predicting fatal outcomes

For historical reasons such as the lack of a sufficiently sized cohort for standard statistical analysis, there is currently no clinical biomarker to predict fatal outcome for lethal burn-hemorrhagic shock combined injury, both in military and civilian populations. We constructed a swine model for burn-hemorrhagic shock combined injury and found that the markedly elevated succinic acid, glutaric acid, and malic acid are closely associated with injury severity, and can efficiently discriminated between mild, moderate and severe disease. Succinic acid, glutaric acid, and malic acid exist in all nucleated cells and they are indeed a likely biomarker that can be used to predict fatal outcome in lethal injury.

## Conclusion

In summary, this study performed an integrated analysis of metabolomic and proteomic data based on the same biological samples from pigs with burn-hemorrhagic shock combined injury. By analyzing the metabolites and protein changes in the acute phase of burn-shock swine model, we are now able to provide a signature and diagnosis proteins and metabolites panel. This panel can predict injury severity and provide a theoretical basis

for early detection of patients who may deteriorate, and reduce the risk of mortality and serious complications of burn/shock combined injury patients.

Despite the difficulties in establishing the burn-hemorrhage shock model and collecting blood samples in the immediate early time post-injury, this important study aids our understanding of how the extreme trauma affects metabolism and multiple pathological processes.

**Acknowledgements**
Not applicable.

**Author contributions**
Y.C., and B.W., wrote the paper; J.H., H.D., S.H., X.Y., W.Z, F.H., Y.Q., X.L., T.L, and Y.W., edited the paper; and B.W. and J.Z, made the figures and analyzed the data; Y.C. and J.C., finalized edits and submission. The all author(s) read and approved the final manuscript.

**Funding**
Not applicable.

**Availability of data and materials**
No datasets were generated or analysed during the current study.

## Declarations

**Ethics approval and consent to participate**
All animal studies were performed in accordance with the Animal Care and Use Committee of the Fourth Medical Center of Chinese People's Liberation Army (PLA) General Hospital.

**Competing interests**
The authors declare no competing interests.

**Author details**
[1]Department of Burns and Plastic Surgery, The Fourth Medical Center of Chinese People's Liberation Army (PLA) General Hospital, Beijing 100048, China. [2]The First Department of Surgery, Chinese People's Armed Police Force Hospital of Beijing, Beijing 100027, China. [3]Institute of Basic Medical Sciences, Chinese Academy of Medical Sciences; School of Basic Medicine, Peking Union Medical College, Beijing 100005, China.

Received: 28 September 2024 Accepted: 19 December 2024
Published online: 07 January 2025

**References**

1. Li Y, et al. Motorcycle accidents in China. Chin J Traumatol. 2008;11(4):243–6.
2. Zou H, et al. The top 5 causes of death in China from 2000 to 2017. Sci Rep. 2022;12(1):8119.
3. Jeschke MG, et al. Burn injury. Nat Rev Dis Primers. 2020;6(1):11.
4. Patti GJ, Yanes O, Siuzdak G. Innovation: metabolomics: the apogee of the omics trilogy. Nat Rev Mol Cell Biol. 2012;13(4):263–9.
5. Trifonova OP, et al. Mass spectrometry-based metabolomics diagnostics—myth or reality? Expert Rev Proteom. 2021;18(1):7–12.
6. Johnson CH, Ivanisevic J, Siuzdak G. Metabolomics: beyond biomarkers and towards mechanisms. Nat Rev Mol Cell Biol. 2016;17(7):451–9.
7. D'Alessandro A, et al. Trauma/hemorrhagic shock instigates aberrant metabolic flux through glycolytic pathways, as revealed by preliminary (13)C-glucose labeling metabolomics. J Transl Med. 2015;13:253.
8. Feng K, et al. Identification of biomarkers and the mechanisms of multiple trauma complicated with sepsis using metabolomics. Front Public Health. 2022;10: 923170.
9. Parent BA, et al. Use of metabolomics to trend recovery and therapy after injury in critically ill trauma patients. JAMA Surg. 2016;151(7): e160853.
10. Hazeldine J, Hampson P, Lord JM. The diagnostic and prognostic value of systems biology research in major traumatic and thermal injury: a review. Burns Trauma. 2016;4:33.
11. Karczewski KJ, Snyder MP. Integrative omics for health and disease. Nat Rev Genet. 2018;19(5):299–310.
12. Munoz B, et al. From traditional biochemical signals to molecular markers for detection of sepsis after burn injuries. Burns. 2019;45(1):16–31.
13. Liang Xi, et al. Serum proteomics reveals disorder of lipoprotein metabolism in sepsis. Life Sci Alliance. 2021;4(10):e202101091. https://doi.org/10.26508/lsa.202101091.
14. Singh A, et al. DIABLO: an integrative approach for identifying key molecular drivers from multi-omics assays. Bioinformatics. 2019;35(17):3055–62.
15. Rohart F, et al. mixOmics: an R package for 'omics feature selection and multiple data integration. PLoS Comput Biol. 2017;13(11): e1005752.
16. Le Boucher J, Cynober L. Protein metabolism and therapy in burn injury. Ann Nutr Metab. 1997;41(2):69–82.
17. Badoiu SC, et al. Glucose metabolism in burns—what happens? Int J Mol Sci. 2021;22(10):5159.
18. Wolfe RR, et al. Glucose metabolism in severely burned patients. Metabolism. 1979;28(10):1031–9.
19. Clayton RP, et al. The effect of burn trauma on lipid and glucose metabolism: implications for insulin sensitivity. J Burn Care Res. 2018;39(5):713–23.
20. Cree MG, et al. Human mitochondrial oxidative capacity is acutely impaired after burn trauma. Am J Surg. 2008;196(2):234–9.
21. Galster AD, et al. Plasma palmitate turnover in subjects with thermal injury. J Trauma. 1984;24(11):938–45.
22. Cree MG, et al. Role of fat metabolism in burn trauma-induced skeletal muscle insulin resistance. Crit Care Med. 2007;35(9 Suppl):S476–83.
23. Lusczek ER, et al. Assessment of key plasma metabolites in combat casualties. J Trauma Acute Care Surg. 2017;82(2):309–16.
24. D'Alessandro A, et al. Plasma succinate is a predictor of mortality in critically injured patients. J Trauma Acute Care Surg. 2017;83(3):491–5.
25. Tretter L, Patocs A, Chinopoulos C. Succinate, an intermediate in metabolism, signal transduction, ROS, hypoxia, and tumorigenesis. Biochim Biophys Acta. 2016;1857(8):1086–101.
26. Slaughter AL, et al. Glutamine metabolism drives succinate accumulation in plasma and the lung during hemorrhagic shock. J Trauma Acute Care Surg. 2016;81(6):1012–9.
27. Reisz JA, et al. Red blood cells in hemorrhagic shock: a critical role for glutaminolysis in fueling alanine transamination in rats. Blood Adv. 2017;1(17):1296–305.
28. Kuriyama N, et al. Bioavailability of reduced coenzyme q10 (ubiquinol-10) in burn patients. Metabolites. 2022. https://doi.org/10.3390/metabo12070613.
29. Nakazawa H, et al. Coenzyme Q10 protects against burn-induced mitochondrial dysfunction and impaired insulin signaling in mouse skeletal muscle. FEBS Open Bio. 2019;9(2):348–63.
30. Garrido-Maraver J, et al. Clinical applications of coenzyme Q10. Front Biosci (Landmark Ed). 2014;19(4):619–33.
31. Minnich A, et al. A potent PPARalpha agonist stimulates mitochondrial fatty acid beta-oxidation in liver and skeletal muscle. Am J Physiol Endocrinol Metab. 2001;280(2):E270–9.
32. Raje V, et al. Adipocyte lipolysis drives acute stress-induced insulin resistance. Sci Rep. 2020;10(1):18166.
33. Adeva-Andany MM, et al. Significance of l-carnitine for human health. IUBMB Life. 2017;69(8):578–94.
34. Chen C, et al. Metabolomic profiling reveals amino acid and carnitine alterations as metabolic signatures in psoriasis. Theranostics. 2021;11(2):754–67.
35. Li P, et al. Exogenous L-carnitine ameliorates burn-induced cellular and mitochondrial injury of hepatocytes by restoring CPT1 activity. Nutr Metab (Lond). 2021;18(1):65.
36. Guasch-Ferre M, et al. Plasma acylcarnitines and risk of type 2 diabetes in a Mediterranean population at high cardiovascular risk. J Clin Endocrinol Metab. 2019;104(5):1508–19.

37. Houck JC, Sharma VK. Induction of collagenolytic and proteolytic activities in rat and human fibroblasts by anti-inflammatory drugs. Science. 1968;161(3848):1361–2.
38. Nemkov T, et al. Red blood cells as an organ? How deep omics characterization of the most abundant cell in the human body highlights other systemic metabolic functions beyond oxygen transport. Expert Rev Proteom. 2018;15(11):855–64.
39. D'Alessandro A, et al. Red blood cell metabolism in vivo and in vitro. Metabolites. 2023. https://doi.org/10.3390/metabo13070793.
40. van Zwieten R, Verhoeven AJ, Roos D. Inborn defects in the antioxidant systems of human red blood cells. Free Radic Biol Med. 2014;67:377–86.
41. Tanzer C, et al. Evaluation of haemoglobin in blister fluid as an indicator of paediatric burn wound depth. Burns. 2015;41(5):1114–21.
42. Bryk AH, Wisniewski JR. Quantitative analysis of human red blood cell proteome. J Proteome Res. 2017;16(8):2752–61.
43. Wu S, et al. BLVRB redox mutation defines heme degradation in a metabolic pathway of enhanced thrombopoiesis in humans. Blood. 2016;128(5):699–709.
44. Paukovich N, et al. Biliverdin reductase B dynamics are coupled to coenzyme binding. J Mol Biol. 2018;430(18 Pt B):3234–50.
45. Bocedi A, et al. Erythrocyte glutathione transferase: a general probe for chemical contaminations in mammals. Cell Death Discov. 2016;2:16029.
46. Ogasawara Y, et al. Structural and functional analysis of native peroxiredoxin 2 in human red blood cells. Int J Biochem Cell Biol. 2012;44(7):1072–7.

## Publisher's Note